CHEMICAL ENGINEERING TRANSACTIONS
VOL. 86, 2021
A publication of AIDIC
The Italian Association of Chemical Engineering
Online at www.cetjournal.it
Guest Editors: Sauro Pierucci, Jiří Jaromír Klemeš
Copyright © 2021, AIDIC Servizi S.r.l.
ISBN 978-88-95608-84-6; **ISSN** 2283-9216

Design and setup activities for the development of methane autothermal reforming in a jet fountain fluidized bed reactor

Simona Renda[a,*], Ferdinando Tommasino[a], Vincenzo Palma[a], Michele Miccio[a], Farouk Okasha[b]

[a]University of Salerno, Department of Industrial Engineering, Via Giovanni Paolo II 132, 84084 Fisciano (SA), Italy
[b]University of Mansoura, Department of Mechanical Power Engineering, Mansoura (Egypt)
srenda@unisa.it

In the framework of hydrogen production and process intensification for energy applications, this work presents the design and the construction of a novel lab-scale experimental facility, which is aimed at testing and demonstrating the feasibility of the auto-thermal catalytic reforming of methane in a recently proposed reactor configuration, i.e., the jetting fountain fluidized bed (JFFBR). The proposed solution consists of a jet pipe and an annulus which are concentrical and it is designed to operate the auto-thermal reforming in two almost-distinct zones: oxidant (oxygen or air) is only fed to the jet pipe, which substantially provides methane partial oxidation and consequently heat generation; the annulus is designed to operate in a bubbling fluidized bed regime, and it is the region in which methane steam reforming essentially occurs. The two zones communicate through a pair of holes in the bottom part of the jet pipe, which determine the entrainment of solid particles and the fountain on the top of the jet pipe. The jetting fountain fluidized bed regime is expected to enhance the heat and mass transfer phenomena, while the selective fed of the oxidant to the jet pipe is expected to provide an in-situ regeneration of the catalyst. In view of starting an actual experimental program with the designed facility, a suitable catalyst has been selected and its catalytic activity has been characterized in a lab-scale fixed-bed reactor. The formulation, previously optimized, involves a ceria-silica support, which can be easily fluidized, and two active phases, namely Ni and Pt, obtaining a final catalyst 3%Pt-10%Ni/CeO_2/SiO_2.The catalyst performed well in terms of activity and selectivity. The activity test results from the fixed-bed reactor allowed to set-up a satisfactory kinetic model of the reacting system.

1. Introduction

The selection of hydrogen as the most promising energy carrier for the future is nowadays widely recognized. The most relevant issues related to its employment are essentially connected to its production: methane reforming is still a high-cost process; furthermore, in order to employ hydrogen as fuel for the automotive sector or in fuel cells, a fully distributed hydrogen production should be achieved (Palma et al., 2019). The most relevant contribution to the total cost of a steam-methane reforming process is the high energy consumption: heat is generated in external burners and has to be transferred to the catalytic bed. A possible solution is to perform instead the catalytic auto-thermal methane reforming (ATR), in which air or pure oxygen is added to the steam reforming mix in order to couple the steam reforming reaction (1) with the methane partial oxidation (2).

$$CH_4 + H_2O \rightleftarrows CO + 3H_2 \qquad \Delta H = 206\ kJ\ mol^{-1} \tag{1}$$

$$CH_4 + \frac{1}{2}O_2 \rightleftarrows CO + 2H_2 \qquad \Delta H = -35.6\ kJ\ mol^{-1} \tag{2}$$

The exothermicity of the partial oxidation enhances the reaction kinetics of the steam reforming and allows the self-sustainability of the overall process (Tariq et al., 2020); furthermore, ATR is preferred also for its better scalability than the conventional reforming process (Blumberg et al., 2019). On the other hand, with the aim of

achieving progressively more compact solutions, the process intensification (PI) of methane reforming is an interesting topic in both scientific and industrial framework. PI of a generic process can be achieved in many different ways: for instance, in catalytic processes one of the most explored routes is the substitution of a conventional catalyst with a high-conductive structured one (Palma et al. 2020). Another important route to PI is pursued when a novel reactor solution is proposed: the jetting fountain fluidized bed reactor (JFFBR) is an innovative configuration that allows an enhanced gas-solid contact with respect to conventional bubbling fluidized bed applications (Okasha, 2016).
With the aim of studying the feasibility of the methane ATR in this particular reactor configuration, a fluidizable catalyst has been chosen on the basis of previous studies (Palma et al., 2018), which is a Pt-Ni catalyst supported on a core-shell structure of CeO_2/SiO_2. Here, silica has been chosen for its fluidizable behaviour and constitutes the core, while CeO_2 has been chosen for its intrinsic ability of avoiding coke deposition and constitutes the shell. Then, several catalytic activity tests have been carried out in order to have a kinetic characterization of the selected formulation in a fixed bed reactor, and a kinetic model with a good agreement with the experimental evaluations has been proposed.

2. ATR design

2.1 Design of the equipment

The JFFBR reactor basically consists of a vertical jet pipe and of an annulus, which are concentrical. The jet pipe is equipped near its bottom with two holes in opposite position, which are responsible for the entrainment of solid particles from the annulus: the fluidizable particles are allowed to enter the holes and are entrained by the gas flowing through the pipe with a high gas velocity; once reached the end of the pipe, the particles are ejected upward and fall back to the annulus when gravity balances the inertia force, creating a fountain shape. In the annulus, a bubbling fluidized regime is maintained.
A schematic representation of the JFFBR is given in Figure 1 (a). For this specific case, a modular JFFBR has been designed as follows. From bottom to top, five external main sections can be distinguished: (i) the pre-mixing chamber, (ii) the ignition chamber, (iii) the reaction zone and the freeboard zone with a cylindrical section (iv) followed by a conic one (v), which mitigates the elutriation of the solid particles. In addition to these, the reactor is constituted by the inner pipe (vi) and two porous sets (vii) respectively placed between sections (i) and (ii) and sections (ii) and (iii). The overall 3D design of the reactor is given in Figure 1 (b) while a cross section is displayed in Figure 1 (c) and (d): the modules that constitute the reactor have been described with arrows.

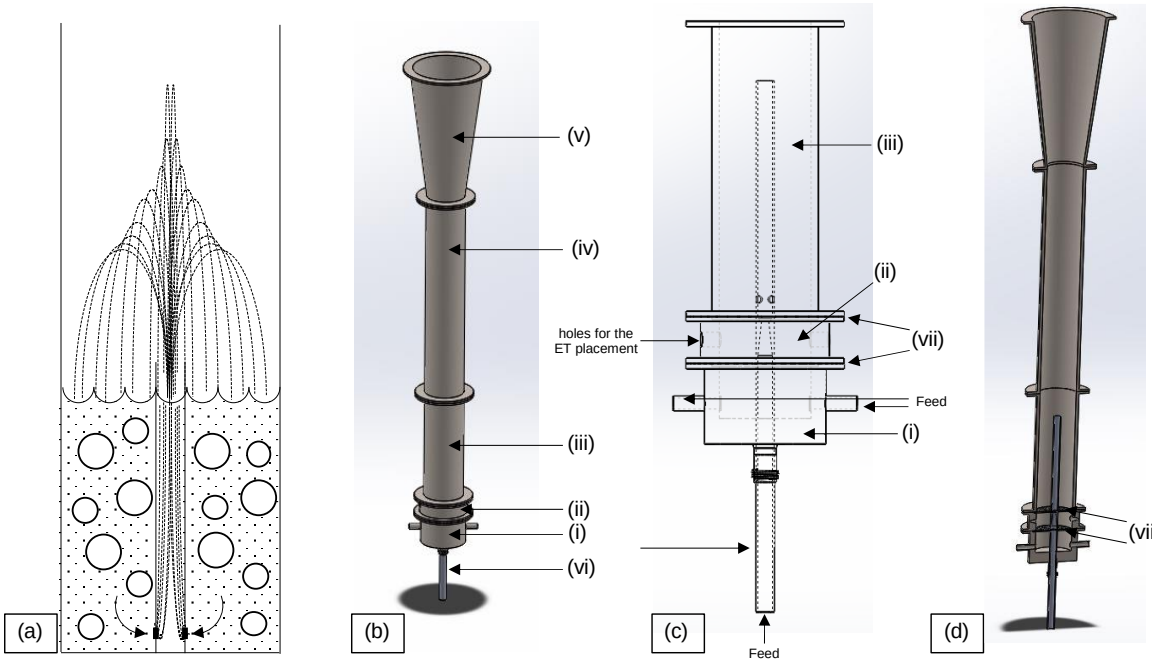

Figure 1: a) Schematic representation of the JFFBR; b) 3D rendering of the reactor; c) and d) cross-sectional view

2.2 Start-up and triggering of the reaction

In order to perform an autothermal reforming process, the exothermic reaction (in this specific case, methane oxidation) needs to be triggered: this defines a precise start-up procedure before ATR can actually start. In a first place, methane is burnt with oxygen or air and the combustion is prompted by means of a couple of electrical triggers (ET) located within module (ii), i.e., the ignition chamber. In this phase, both reactants are fed to the pre-mixing chamber (i) located upstream. Once combustion starts to take place, the temperature progressively increases and the hot combustion products flow within the downstream modules, heating the whole system. Once a suitable temperature (above 800°C) is reached in the catalytic module (reaction zone, iii), the start-up procedure is completed, and it is possible to switch to the steady-state operating mode.

2.3 Steady-state operating mode

The auto-thermal reforming is performed within the inner pipe and the annulus. Methane and steam are fed to the pre-mixing chamber (i) and then proceed up to the reactor to reach the annulus which is the reacting zone (iii) and provides for the fluidization of the catalyst. Module (i) realizes an adequate mixing of the reactants, in order to reach an almost plug-flow profile of linear velocity before the downstream sections: this is particularly important in order to achieve a homogeneous fluidization of the catalytic bed.
Oxygen (or air) is fed to the inner pipe (vi) and is responsible of the jetting fountain effect: the entrance of the solid particles within the holes is even enhanced by the presence of a section contraction just before the holes, which ensures a Venturi-type effect, creating a depression in the hole surroundings and thus determining a suction of the solid particles.
Despite methane and steam are fed to the catalyst from the bottom while the oxidant is substantially fed to the inner pipe, the continuous mixing reached in the fluidized bed ensures both heat and mass transport to be adequate. Furthermore, the oxygen-rich atmosphere within the inner pipe is particularly suitable to provide a fast regeneration of the catalyst, when considering the possible deposition of coke on the metallic sites of catalytic particles.

3. Preliminary catalytic evaluations

3.1 Catalyst preparation and characterization

The Pt-Ni/CeO_2/SiO_2 catalyst was prepared as follows. Mesoporous silica (Sigma-Aldrich) was calcined at 900°C for 3 h and then added to a solution of $Ce(NO_3)\cdot 6H_2O$ (Strem Chemicals) in bi-distilled water for Ce deposition: the amount of cerium precursor salt dissolved in water was determined in order to achieve a Ce loading of 30%wt with respect to silica. The suspension was kept stirring at 80°C until total water evaporation, then the catalyst was dried overnight at 120°C and calcined under the same previous conditions (900°C, 3h).
Nickel and platinum were added in this order in two subsequent impregnation steps, using $Ni(NO_3)_2\cdot 6H_2O$ and $PtCl_4$ as precursor salts (Sigma-Aldrich both), determining the salts amount in order to achieve a loading of 10%wt and 3%wt of the CeO_2 loading, respectively for Ni and Pt. After each impregnation step, the catalyst was dried and calcined as above described.
The specific surface area (SSA) of the catalyst was evaluated with a Costech International Sorptometer 1040 by N_2 dynamic adsorption at –196°C and the SSA value was given by the B.E.T. equation. The reducibility properties of the catalyst were evaluated with a temperature programmed reduction (TPR) procedure performed in-situ before each catalytic test: the analysis was performed with a reducing stream (500 Ncm^3/min, 5%H_2 in N_2), increasing the temperature with a heating rate of 10 °C/min up to 900°C.

3.2 Operating procedure

The activity tests were performed in a fixed bed reactor, in order to perform a preliminary, but necessary kinetic study on the catalyst. A tubular reactor (stainless-steel AISI 310, 380 mm long and with an internal diameter of 22 mm) was employed, and it was horizontally located in an electric furnace for heat supply. Two K-type thermocouples were employed to monitor the temperature at the inlet and outlet of the catalytic bed; in the inlet section, the reactor was equipped with an internal coil (1/8” ID and 400 mm long) for water vaporization. 2 g of catalysts (particle size in the range 180-355 μm) was loaded in the middle of the reactor, diluted with quartz spheres (500-710 μm) with a 1:1 dilution ratio and held between two quartz wool disks. The product stream was dehydrated in a cold trap (2°C) and then sent to a mass spectrometer (Hiden Analytical) for a continuous analysis. The activity tests were carried out in the temperature range 700-950°C by decreasing the temperature in steps; the feed ratio was CH_4:O_2:H_2O = 1:0.6:1. In order to perform a detailed kinetic evaluation, the tests were conducted at three different space velocity values (GHSV, defined as the ratio between the gas flow rate and the catalyst volume), namely 12000, 18000 e 24000 h^{-1}.

3.3 Characterization and activity test results

The results of the SSA analysis are reported in Figure 2 (a). As it is possible to see, the specific surface area available on the catalyst (S_{BET}) is lowered by the addition of CeO_2 and the active metals, even if the greatest contribution to the decrease of the S_{BET} value is determined by the calcination: in fact, the very high calcination temperature (900°C) induced structural modifications in the mesoporous silica. The reduction profile obtained for the catalyst is displayed in Figure 2 (b). The lowest temperature reduction peaks (251 and 390°C) are ascribable to PtO_2 and NiO respectively, while the peak at 580°C can be attributed to the superficial CeO_2 reduction. The sharp peak observed at 762°C and its shoulder at 810°C can be ascribed to the stepwise reduction of ceria, which is strongly bonded to SiO_2 by elimination of O^{2-} anions of the lattice due to formation of Ce_2O_3 (Gao et al., 2008).

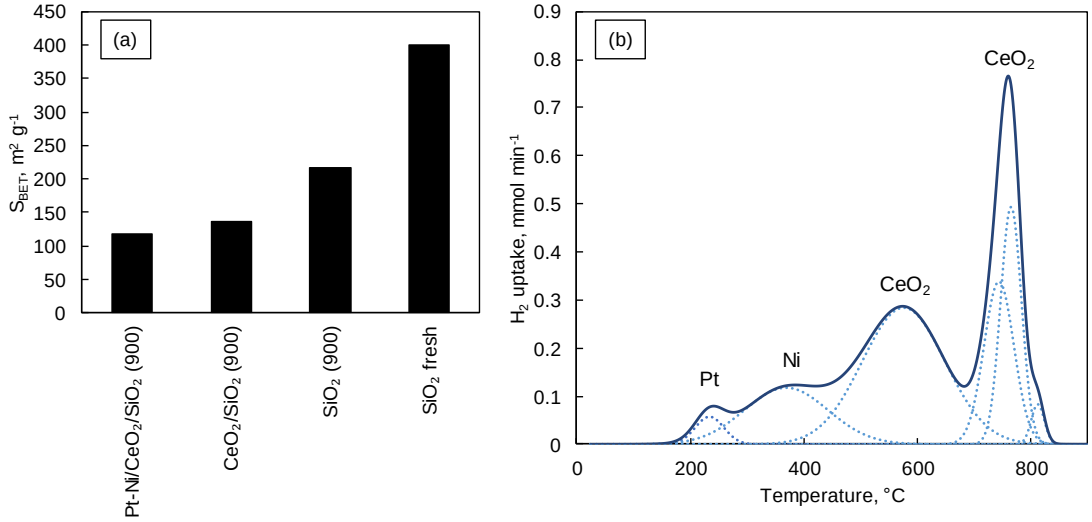

Figure 2: Characterization results: a) S_{BET} values; b) Hydrogen consumption during TPR analysis

Methane conversion as a function of temperature for the three GHSV considered is displayed in Figure 3. As it is possible to see, the conversion values decrease with the decrease of temperature and with the increase of the GHSV. The most relevant outcome, considering the aim of these experimental evaluations, is that the chosen formulation was found to be suitable to catalyze the auto-thermal reforming reaction, even if it was not optimized for this specific process.

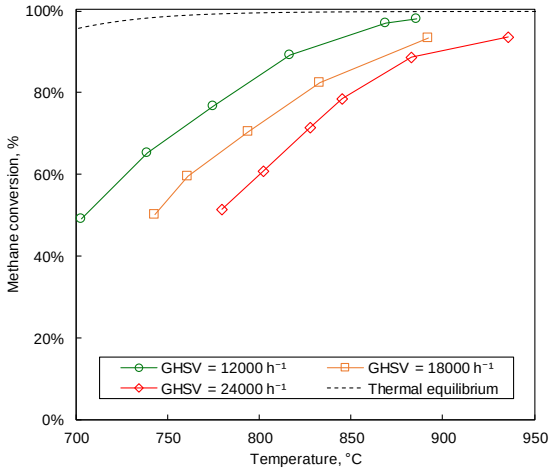

Figure 3: Methane conversion as a function of temperature and GHSV

3.4 Kinetic model

The results obtained from the activity tests were employed to set up a kinetic model to describe the behavior of the selected catalyst. To this aim, three linearly independent reactions have been considered: methane steam reforming (3), CO water-gas shift (4) and methane combustion (5).

$$CH_4 + H_2O \rightleftarrows CO + 3H_2 \quad (3)$$

$$CO + H_2O \rightleftarrows CO_2 + H_2 \quad (4)$$

$$CH_4 + 2O_2 \rightleftarrows CO_2 + 2H_2O \quad (5)$$

The kinetic parameters (pre-exponential factor, k_0, and activation energy, E_a) were optimized through the Euler method by minimizing an error function defined as (6) where y_i is the molar concentration of the i-species evaluated experimentally (exp) or through the model (mod).

$$f = \min\left(\sum_{i=1}^{n}(y_{i,exp} - y_{i,mod})^2\right) \quad (6)$$

The reaction rates of methane steam reforming (SR) and CO water-gas shift (WGS) given by Turchetti et al., (2016) were adopted here. Their expressions are respectively defined as equation (7) and (8); kinetic constant and equilibrium constant were given respectively in equation (9) and (10) as a function of temperature. Parameters A, B and α for the equilibrium constants were obtained through the software GasEq and are listed in Table 1.

$$r_{SR} = k_{SR} p_{CH_4}\left(1 - \frac{p_{CO}p_{H2}^3}{p_{CH4}p_{H2O}}\frac{1}{P_{ref}^2}\frac{1}{K_{SR}}\right) \quad (7)$$

$$r_{WGS} = k_{WGS} p_{CO}\left(1 - \frac{p_{CO2}p_{H2}}{p_{CO}p_{H2O}}\frac{1}{K_{WGS}}\right) \quad (8)$$

$$k_i = k_{0,i} \cdot e^{-E_a/R \cdot T} \quad (9)$$

$$K_{eq,i} = A \cdot T^{\alpha} \cdot e^{B/T} \quad (10)$$

Table 1: Parameters for equilibrium constants determination

	A (K^{-1})	B (K)	α
SR	$4.527 \cdot 10^{14}$	$-2.478 \cdot 10^{4}$	2.51
WGS	$8.64 \cdot 10^{7}$	$5.457 \cdot 10^{3}$	1.28

Methane oxidation occurs almost instantaneously and, as result, no oxygen was ever detected in the products stream analyzed via the mass spectrometer. Considering this, it was not possible to estimate the kinetic behavior of reaction (5): therefore, in order to take into account the methane consumed by this reaction, the material balance was considered. The rate of formation/consumption for each species can be then expressed as follows:

$$CH_4 = -r_{SR} - \frac{1}{2}O_2 \quad (11)$$

$$CO = r_{SR} - r_{WGS} \quad (12)$$

$$H_2 = 3r_{SR} + r_{WGS} \quad (13)$$

$$H_2O = -r_{SR} - r_{WGS} \quad (14)$$

$$CO_2 = r_{WGS} \quad (15)$$

The optimization of the kinetic parameters led to the results reported in Table 2. These parameters allowed the obtainment of a model that gives a satisfactory representation of the experimental data. A comparison of the experimental results and the predicted concentrations is given in Figure 4. The kinetic characterization of the catalyst will be important in the forthcoming activities, in which the first experimental tests will be performed in

the JFFBR. This preliminary activity will contribute to discriminate the enhancing effect of the fluidized regime with respect to the conventional fixed bed application.

Table 2: Optimized kinetic parameters for the catalyst Pt-Ni/CeO_2/SiO_2 and statistic performance indexes

	K_0 (mol Pa^{-1} g^{-1}_{cat} s^{-1})	E_a (J mol^{-1})		12000 h^{-1}	18000 h^{-1}	24000 h^{-1}
SR	$5.01 \cdot 10^{-3}$	$1.28 \cdot 10^{5}$	r^2	71%	70%	42%
WGS	$1.36 \cdot 10^{-4}$	$1.43 \cdot 10^{5}$	f_{min} (eq.6) $(\%)^2$	85	51	88
			SSE $(\%)^2$	17	10	17.7

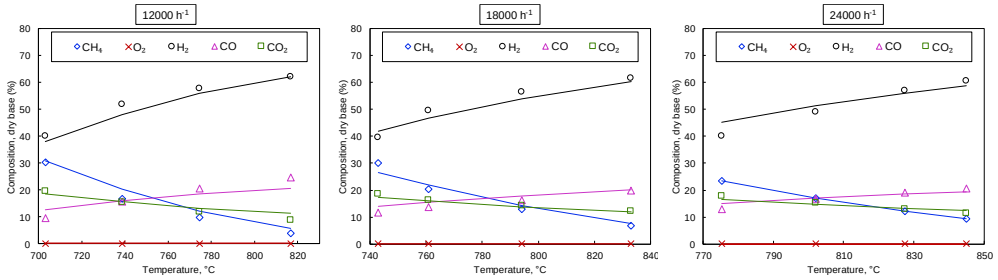

Figure 4: Comparison between experimental (symbols) and predicted (straight lines) concentration values in the three condition of GHSV investigated

4. Conclusions

In this work, the design of a novel reactor for the auto-thermal reforming of methane was presented. The technology, known as jetting fountain fluidized bed reactor, is particularly promising for the ATR reaction, as it is able to enhance the heat and mass transport phenomena. Heat transfer enhancement is fundamental in this kind of process, because of the coupling of the exothermic and endothermic reactions. With the aim of approaching an experimental campaign of catalytic activity tests in the JFFBR, a catalyst previously optimized for a different process has been selected for its fluidizable properties, and tested in a fixed bed reactor in order to evaluate: (i) whether the formulation might be effective in catalyze this reaction and (ii) the kinetic parameters specific for the selected catalyst. As result, the catalyst was found to be promising even at the highest space velocity considered, so that it can be used in the forthcoming activities in the JFFBR. Furthermore, the kinetic parameters optimized in this study allowed to obtain a satisfactory description of the catalytic behavior observed experimentally. These results are only preliminary, but very promising to the aim of performing the ATR of methane in the JFFBR.

References

Blumberg T., Lee Y.D., Morosuk T., Tsatsaronis G., 2019, Exergoenvironmental analysis of methanol production by steam reforming and autothermal reforming of natural gas, Energy, 181, 1273-1284.

Gao J., Guo J., Liang D., Hou Z., Fei J., Zheng X., 2008, Production of syngas via autothermal reforming of methane in a fluidized-bed reactor over the combined CeO_2–ZrO_2/SiO_2 supported Ni catalysts, International Journal of Hydrogen Energy, 33(20), 5493-5500.

Okasha F.M., 2016, Short overview on the jetting-fountain fluidized bed (JFFB) combustor, Renewable and Sustainable Energy Reviews, 55, 674-686.

Palma V., Barba D., Meloni E., Renda S., Ruocco C., 2019, Ultracompact biofuels catalytic reforming processes for distributed renewable hydrogen production, Studies in Surface Science and Catalysis, 179, 317-333.

Palma V., Meloni E., Renda S., Martino M., 2020, Catalysts for Methane Steam Reforming Reaction: Evaluation of CeO_2 Addition to Alumina-Based Washcoat Slurry Formulation, C – Journal of Carbon Research, 6, 52.

Palma V., Ruocco C., Ricca A., 2018, Oxidative steam reforming of ethanol in a fluidized bed over CeO_2-SiO_2 supported catalysts: effect of catalytic formulation, Renewable Energy, 125, 356-364.

Tariq R., Maqbool F., Abbas S.Z., 2020, Small-scale production of hydrogen via auto-thermal reforming in an adiabatic packed bed reactor: Parametric study and reactor's optimization through response surface methodology, Computers & Chemical Engineering, in press, 107192.

Turchetti L., Murmura M.A., Monteleone F., Giaconia A., Lemonidou A.A., Angeli S.D., Palma V., Ruocco C., Annesini M.C., 2016, Kinetic assessment of Ni-based catalysts in low-temperature methane/biogas steam reforming, International Journal of Hydrogen Energy, 41(38), 16865-16877.